Calculations of 2p lifetimes in the Li sequence

Constantine E. Theodosiou and Lorenzo J. Curtis

Department of Physics and Astronomy, University of Toledo, Toledo, Ohio 43606

Mohammed El-Mekki

Department of Chemistry, University of Toledo, Toledo, Ohio, 43606

(Received 21 June 1991)

Lifetime predictions for the $2p\,{}^2P_{1/2}$ and $2p\,{}^2P_{3/2}$ levels in the lithium isoelectronic sequence have been computed for atomic numbers $Z=3\text{--}92$ using the semiempirical Coulomb approximation with a Hartree-Slater core. This extends our earlier studies of the sodium and copper sequences, and the results agree well with critically selected experimental lifetime measurements. The calculations involve the inclusion of experimental energy level, ionization potential, and core-polarizability data, and we also report here a comprehensive and reliable data base developed through semiempirical parametrizations of spectroscopic measurements and *ab initio* calculations.

PACS number(s): 32.70.Fw, 31.50.+w

I. INTRODUCTION

The ns-np resonance transitions in alkali-metal-like isoelectronic sequences can provide important tests of theoretical methods and experimental measurements. As one example, lifetime measurements for these transitions can be used to determine whether wave functions constructed to optimize the specification of energy levels also optimize the prediction of transition probabilities. Although the alkali-metal-like systems consist primarily of a single electron outside closed shells, these intrashell resonance transitions involve theoretical and experimental subtleties. Theoretical calculations must properly include electron correlation, spin-orbit coupling, and relativistic interactions, whereas experimental measurements must take into account repopulation both from fast growing-in extrashell cascades and from slow growing-out cascades from the yrast chain. As another example, at high nuclear charge Z, these transitions sensitively test quantum electrodynamical (QED) self-energy corrections. Although the QED corrections to these many-body systems are more complicated than hydrogenlike systems theoretically, they possess many attractive experimental features. By virtue of the $\Delta n = 0$ nature of these resonance transitions, they have lower excitation energies (and are more easily populated), longer wavelengths (and are more easily detected), and longer lifetimes (and can be more easily studied by impulsive excitation) than hydrogenlike resonance transitions at the same value of Z.

The lifetimes of the 2s-2p resonance transitions in the Li sequence have been computed by a variety of methods [1–9], and experimental measurements exist for a number of ions [10–29]. Some discrepancies have been noted, and questions have been raised as to whether theoretical and experimental uncertainties can overlap in the case of neutral lithium [4]. In earlier studies of the Na [30] and Cu [31] isoelectronic sequences, we constructed semiempirical wave functions from spectroscopic data using the Coulomb approximation with a realistic model poten-

tial [30–35]. These studies yielded lifetime predictions that often agreed more closely with experimental values than did results using *ab initio* methods. We report an extension of this approach to the Li sequence. In order to carry out this calculation, it was necessary to develop a reliable and comprehensive data base of spectroscopic energy levels, ionization potentials, and core-polarization parameters for this isoelectronic sequence, which we obtained through the combined use of available measured data, *ab initio* calculations, and semiempirical parametrizations.

II. DATA BASE

As is discussed in Sec. III, the semiempirical methods used here generate wave functions from spectroscopic data, and require as input precise values for the excitation energies of the decaying levels and the ionization potential of the ground state, as well as the dipole polarizability of the heliumlike core. Precision measurements for excitation energies are available for selected ions in the Li sequence through 90 stages of ionization [36–41], and it has been demonstrated [42] that these data can be parametrized to obtain reliable interpolative and extrapolative predictions. Extrapolation formulas are also available for the ionization potentials [43], as are theoretical compilations of the core polarizabilities [44].

To obtain reliable values for the excitation energies, we have used a combination of theoretical calculations and empirical data parametrizations. Precise calculations for the electron-nucleus and electron-electron energies for ions in the Li isoelectronic sequence have recently been reported by Johnson *et al.* [45,46] using relativistic many-body perturbation theory (RMBPT) and by Indelicato *et al.* [47] using multiconfiguration Dirac-Fock (MCDF) methods. Although these two calculations predict slightly different contributions for electrostatic electron correlation at high Z, the primary uncertainty in the total energy lies in the specification of the electron self-

energy corrections for this three-body system, often designated as the "screening of the Lamb shift."

Various attempts to specify these QED corrections have been made. Desclaux, Cheng, and Kim [48] and Grant and co-workers [49] have constructed order-of-magnitude estimates within their computer codes that are based on a screened hydrogenlike model. These codes approximate many-body self-energy corrections by interpolating the numerical tabulations [50] of these corrections for hydrogenlike ions using an effective screened nuclear charge. The effective charge for each orbital is defined by requiring that a hydrogenlike ion with this screened nuclear charge will yield an identical expectation value for the orbit radius. Clearly the expectation values of the Lamb-shift operator and of the radial coordinate emphasize quite different portions of the wave function, and this approximation should be regarded with caution. These codes have been applied to estimate the QED corrections to the Li sequence by Cheng, Kim, and Desclaux [3] and by Seely [51], but the validity of these screening models is untested. Indelicato and Desclaux [47] have made specific QED calculations for the Li system, but where comparisons exist their results seem to overestimate the screening slightly [41]. Curtis [42] has left the effective QED hydrogenlike screening as a free parameter to be specified and extrapolated empirically. Since our goal is to obtain the highest possible precision by empirical rather than *ab initio* methods, we have used the semiempirical method of Ref. [42] to develop the data base used here.

Following the approach of Ref. [42], we have made a semiempirical adjustment of the *ab initio* RMBPT calculations (with nuclear penetration corrections) for the $2s\,^2S_{1/2}-2p\,^2P_{1/2}$ "irregular doublet" and $2p\,^2P_{1/2}-2p\,^2P_{3/2}$ "regular doublet" intervals for the Li sequence reported by Johnson, Blundell, and Sapirstein [45,46]. These calculations include all interactions except for the Lamb shift (i.e., the one-electron self-energy, the vacuum polarization, and other QED corrections), and effective values for the Lamb shifts for these intervals can be obtained by subtracting the predictions from the corresponding observed data. The empirical data reduction presented in Ref. [42] maps these residues into a screening parameter defined by the Z-interpolated value Z_s that causes the hydrogenic Lamb shift [52] to equal the residue. A comparison of Refs. [45] and [47] indicates that a portion of this residue may arise from correlation and other non-QED contributions, so this effective screening should be used only for semiempirical predictions, and may not correspond to *ab initio* definitions of the screening of the Lamb shift.

An isoelectronic plot of the effective screening parameter for the Lamb shift of the irregular-doublet interval is shown in Fig. 1. Experimental uncertainties (propagated from quoted wavelength uncertainties) are indicated by error bars. For $Z \leq 7$ the QED corrections are small, and other perturbations may distort the residues and reduce the effective screening. For $8 \leq Z \leq 92$ the screening is
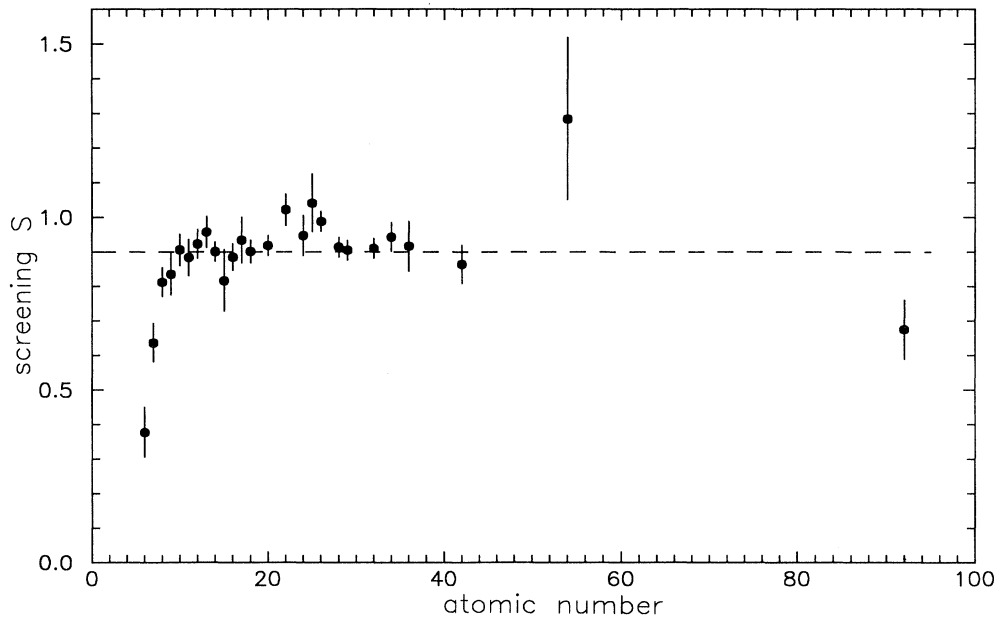

FIG. 1. Screening parametrization of the $2s$-$2p_{1/2}$ Lamb shift. The ordinate denotes the amount by which the charge of a hydrogenlike ion must be reduced so that its QED corrections [52] equal the residue between the measured [36–39] and theoretically computed [45,46] values for this interval.

TABLE I. Predictions of the resonance transition wavelengths (in vacuum Å) for the Li sequence using the theoretical calculations of Refs. [45] and [46] and the screening parametrization of the hydrogenlike Lamb shift of Ref. [42]. The screening parameters $Z - Z_s = 0.9$ and 1.4 were used for the irregular- and regular-doublet intervals. These predictions are compared with observed values, with quoted uncertainties indicated in parentheses.

Ion	Z	$\lambda(\frac{1}{2} - \frac{1}{2})$ Predicted	Observed	$\lambda(\frac{1}{2} - \frac{3}{2})$ Predicted	Observed	Reference
Li	3		6709.764		6709.613	a
Be	4		3131.973		3131.327	a
B	5		2067.893		2066.436	a
C	6	1550.63	1550.772(24)	1548.04	1548.196(24)	a
N	7	1242.74	1242.807(15)	1238.74	1238.820(15)	a
O	8	1037.59	1037.613(11)	1031.89	1031.928(11)	a
F	9	890.765	890.781(16)	883.082	883.104(16)	a
Ne	10	780.332	780.329(12)	770.397	770.416(12)	a
Na	11	694.142	694.146(14)	681.705	681.696(23)	a
Mg	12	624.960	624.953(12)	609.785	609.804(11)	a
Al	13	568.160	568.143(13)	550.032	550.031(15)	a
Si	14	520.668	520.668(8)	499.395	499.406(10)	a
P	15	480.351	480.377(28)	455.768	455.741(31)	a
S	16	445.682	445.686(12)	417.651	417.648(9)	a
Cl	17	415.537	415.526(21)	383.952	383.982(22)	a
Ar	18	389.075	389.075(11)	353.863	353.867(13)	a
K	19	365.663		326.780		
Ca	20	344.777	344.771(10)	302.217	302.208(9)	a
Sc	21	326.029		279.817		
Ti	22	309.106	309.065(15)	259.297	259.300(20)	b
V	23	293.749		240.428		
Cr	24	279.745	279.729(20)	223.024	223.010(20)	b
Mn	25	266.919		206.935		
Fe	26	255.125	255.094(10)	192.037	192.012(20)	b
Co	27	244.240		178.225		
Ni	28	234.160	234.155(10)	165.411	165.396(10)	b
Cu	29	224.797	224.795(10)	153.517	153.507(20)	b
Zn	30	216.073		142.474		
Ga	31	207.923		132.222		
Ge	32	200.294	200.290(10)	122.707	122.705(20)	b
As	33	193.129		113.876		
Se	34	186.390	186.375(15)	105.685	105.686(20)	b
Br	35	180.043		98.092		
Kr	36	174.042	174.036(26)	91.052	91.049(25)	b
Rb	37	168.368		84.530		
Sr	38	163.000		78.492		
Y	39	157.904		72.901		
Zr	40	153.048		67.723		
Nb	41	148.406		62.926		
Mo	42	143.985	143.998(20)	58.488	58.499(20)	b
Tc	43	139.791		54.390		
Ru	44	135.799		50.602		
Rh	45	131.987		47.100		
Pd	46	128.339		43.859		
Ag	47	124.838		40.859		
Cd	48	121.469		38.082		
In	49	118.221		35.508		
Sn	50	115.086		33.124		
Sb	51	112.051		30.913		
Te	52	109.110		28.862		
I	53	106.256		26.958		
Xe	54	103.483	103.35(8)	25.192	25.18(3)	c
Cs	55	100.804		23.554		
Ba	56	98.231		22.038		
La	57	95.755		20.634		

TABLE I. (Continued).

Ion	Z	$\lambda(\frac{1}{2}-\frac{1}{2})$ Predicted	$\lambda(\frac{1}{2}-\frac{1}{2})$ Observed	$\lambda(\frac{1}{2}-\frac{3}{2})$ Predicted	$\lambda(\frac{1}{2}-\frac{3}{2})$ Observed	Reference
Ce	58	93.371		19.331		
Pr	59	91.072		18.123		
Nd	60	88.854		16.999		
Pm	61	86.711		15.955		
Sm	62	84.638		14.983		
Eu	63	82.632		14.078		
Gd	64	80.686		13.235		
Tb	65	78.805		12.448		
Dy	66	76.977		11.714		
Ho	67	75.204		11.028		
Er	68	73.480		10.387		
Tm	69	71.806		9.787		
Yb	70	70.178		9.225		
Lu	71	68.593		8.699		
Hf	72	67.053		8.206		
Ta	73	65.552		7.744		
W	74	64.091		7.311		
Re	75	62.671		6.904		
Os	76	61.293		6.522		
Ir	77	59.957		6.165		
Pt	78	58.663		5.829		
Au	79	57.407		5.515		
Hg	80	56.188		5.219		
Tl	81	55.006		4.941		
Pb	82	53.868		4.680		
Bi	83	52.748		4.435		
Po	84	51.670		4.204		
At	85	50.624		3.987		
Rn	86	49.608		3.782		
Fr	87	48.622		3.590		
Ra	88	47.666		3.408		
Ac	89	46.738		3.237		
Th	90	45.837		3.076		
Pa	91	44.962		2.924		
U	92	44.112	44.170(22)	2.780		d

[a]Edlén (compilation) Refs. [36] and [43].
[b]Hinnov and Denne, Ref. [37].
[c]Martin et al. Ref. [38].
[d]Schweppe, Ref. [39].

well represented by a constant value 0.9. For the regular doublet the relative magnitude of the Lamb shift is smaller, but a similar plot can be made, albeit with larger relative uncertainties. In Ref. [42] these screening parameters were approximated by $Z-Z_s=0.9$ and 1.4 for the irregular and regular doublets, respectively. In the intervening 2 years, the scope and accuracy of the data has increased, providing further confirmation of these approximations. Blundell, Johnson, and Sapirstein have recently made similar estimates [46] of these quantities as 0.956 and 1.422. If the values for the Lamb shift generated by Seely [51] using the Grant program [49] are converted to hydrogenlike screening parameters, these quantities can be represented by $Z-Z_s=0.94-0.7(\alpha Z)^4$ and $1.6-8(\alpha Z)^2$ for the irregular- and regular-doublet intervals. These values are similar to those obtained sem-

iempirically, but since the basis of the approximation used in the Grant program is questionable, we have used the effective screening parameters obtained from the measured data [42] in our extrapolations here.

The resonance-transition-wavelength predictions of Ref. [42] are reproduced and extended in Table I, where they are also compared with available measurements, with experimental uncertainties and source references indicated. The measurements of Hinnov and Denne [37] were performed subsequent to and with the aid of these predictions, and they constitute strong confirmation (to within accuracies as high as parts in 10^6) of this semiempirical approach. Another measurement for $Z=36$ has recently been made [40] which disagrees with Ref. [37], but the isoelectronic trend [41] favors the value of Ref. [37]. The results are also compared with measure-

TABLE II. Compilation of excitation energies and ionization potentials (IP) (in cm^{-1}) and dipole polarizabilities (in a_0^3) for the Li isoelectronic sequence.

Ion	Z	$P_{1/2}$[a]	$P_{3/2}$[a]	IP[b]	α_d[c]
Li	3	14 903.7	14 904.0	43 487	1.894×10^{-1}
Be	4	31 928.7	31 935.3	146 883	5.182×10^{-2}
B	5	48 358	48 392	305 931	1.953×10^{-2}
C	6	64 484	64 591	520 180	8.919×10^{-3}
N	7	80 463	80 722	789 537	4.633×10^{-3}
O	8	96 375	96 906	1 114 004	2.639×10^{-3}
F	9	112 261	113 237	1 493 622	1.611×10^{-3}
Ne	10	128 151	129 800	1 928 449	1.038×10^{-3}
Na	11	144 062	146 693	2 418 574	6.986×10^{-4}
Mg	12	160 012	163 987	2 964 085	4.870×10^{-4}
Al	13	176 012	181 808	3 565 097	3.497×10^{-4}
Si	14	192 061	200 238	4 221 723	2.575×10^{-4}
P	15	208 170	219 423	4 934 105	1.937×10^{-4}
S	16	224 373	239 436	5 702 379	1.485×10^{-4}
Cl	17	240 659	260 429	6 526 714	1.156×10^{-4}
Ar	18	257 020	282 592	7 407 274	9.138×10^{-5}
K	19	273 476	306 016	8 344 225	7.314×10^{-5}
Ca	20	290 048	330 898	9 337 781	5.922×10^{-5}
Sc	21	306 721	357 376	10 388 154	4.844×10^{-5}
Ti	22	323 557	385 654	11 495 547	3.999×10^{-5}
V	23	340 427	415 926	12 660 200	3.329×10^{-5}
Cr	24	357 489	448 410	13 882 352	2.793×10^{-5}
Mn	25	374 714	483 348	15 162 273	2.360×10^{-5}
Fe	26	392 012	520 801	16 500 226	2.007×10^{-5}
Co	27	409 434	561 087	17 896 511	1.717×10^{-5}
Ni	28	427 068	604 610	19 351 412	1.477×10^{-5}
Cu	29	444 850	651 436	20 865 272	1.277×10^{-5}
Zn	30	462 807	701 884	22 438 396	1.110×10^{-5}
Ga	31	480 948	756 307	24 071 150	9.665×10^{-6}
Ge	32	499 276	814 963	25 763 883	8.464×10^{-6}
As	33	517 790	878 148	27 516 977	7.455×10^{-6}
Se	34	536 553	946 199	29 330 833	5.943×10^{-6}
Br	35	555 424	1 019 450	31 205 852	5.839×10^{-6}
Kr	36	574 594	1 098 310	33 142 479	5.189×10^{-6}
Rb	37	593 938	1 183 018	35 141 148	4.626×10^{-6}
Sr	38	613 496	1 274 012	37 202 333	4.132×10^{-6}
Y	39	633 295	1 371 714	39 326 517	3.705×10^{-6}
Zr	40	653 390	1 476 605	41 514 208	3.332×10^{-6}
Nb	41	673 829	1 589 181	43 765 929	3.001×10^{-6}
Mo	42	694 454	1 709 431	46 082 230	2.710×10^{-6}
Tc	43	715 356	1 838 573	48 463 670	2.450×10^{-6}
Ru	44	736 385	1 976 198	50 910 855	2.212×10^{-6}
Rh	45	757 650	2 123 165	53 424 378	2.019×10^{-6}
Pd	46	779 188	2 280 040	56 004 891	1.838×10^{-6}
Ag	47	801 040	2 447 421	58 653 041	1.676×10^{-6}
Cd	48	823 254	2 625 935	61 369 530	1.531×10^{-6}
In	49	845 867	2 816 228	64 155 055	1.400×10^{-6}
Sn	50	868 916	3 018 988	67 010 364	1.283×10^{-6}
Sb	51	892 449	3 234 933	69 936 217	1.177×10^{-6}
Te	52	916 503	3 464 810	72 933 418	1.082×10^{-6}
I	53	941 120	3 709 410	76 002 768	9.957×10^{-7}
Xe	54	966 345	3 969 557	79 145 152	9.173×10^{-7}
Cs	55	992 022	4 245 520	82 361 436	8.462×10^{-7}
Ba	56	1 018 012	4 537 532	85 652 554	7.815×10^{-7}
La	57	1 044 334	4 846 386	89 019 444	7.221×10^{-7}
Ce	58	1 070 999	5 172 912	92 463 102	6.686×10^{-7}
Pr	59	1 098 027	5 517 998	95 984 456	6.201×10^{-7}
Nd	60	1 125 439	5 882 560	99 584 860	5.761×10^{-7}
Pm	61	1 153 259	6 267 574	103 265 119	5.359×10^{-7}

TABLE II. (Continued).

Ion	Z	$P_{1/2}$[a]	$P_{3/2}$[a]	IP[b]	α_d[c]
Sm	62	1 181 504	6 674 056	107 026 480	4.989×10^{-7}
Eu	63	1 210 187	7 103 077	110 870 110	4.642×10^{-7}
Gd	64	1 239 333	7 555 767	114 797 249	4.314×10^{-7}
Tb	65	1 268 963	8 033 308	118 809 151	3.997×10^{-7}
Dy	66	1 299 084	8 536 946	122 907 140	3.702×10^{-7}
Ho	67	1 329 722	9 067 999	127 092 572	3.439×10^{-7}
Er	68	1 360 909	9 627 857	131 366 862	3.205×10^{-7}
Tm	69	1 392 639	10 217 957	135 731 470	2.996×10^{-7}
Yb	70	1 424 945	10 839 847	140 187 912	2.808×10^{-7}
Lu	71	1 457 862	11 495 158	144 737 751	2.636×10^{-7}
Hf	72	1 491 355	12 185 547	149 382 616	2.476×10^{-7}
Ta	73	1 525 500	12 912 861	154 124 184	2.324×10^{-7}
W	74	1 560 285	13 678 950	158 964 200	2.176×10^{-7}
Re	75	1 595 644	14 484 936	163 904 464	2.036×10^{-7}
Os	76	1 631 511	15 331 692	168 946 848	1.909×10^{-7}
Ir	77	1 667 846	16 220 884	174 093 279	1.793×10^{-7}
Pt	78	1 704 654	17 154 242	179 345 759	1.684×10^{-7}
Au	79	1 741 961	18 133 561	184 706 361	1.582×10^{-7}
Hg	80	1 779 747	19 160 708	190 177 233	1.486×10^{-7}
Tl	81	1 817 969	20 237 499	195 760 592	1.397×10^{-7}
Pb	82	1 856 384	21 365 915	201 458 732	1.313×10^{-7}
Bi	83	1 895 801	22 548 281	207 274 029	1.234×10^{-7}
Po	84	1 935 342	23 786 037	213 208 945	1.162×10^{-7}
At	85	1 975 366	25 081 853	219 266 030	1.093×10^{-7}
Rn	86	2 015 803	26 437 728	225 447 931	1.028×10^{-7}
Fr	87	2 056 663	27 856 026	231 757 339	9.665×10^{-8}
Ra	88	2 097 917	29 338 981	238 197 089	9.089×10^{-8}
Ac	89	2 139 578	30 889 080	244 770 094	8.552×10^{-8}
Th	90	2 181 654	32 508 825	251 479 382	8.054×10^{-8}
Pa	91	2 224 114	34 200 693	258 328 048	7.595×10^{-8}
U	92	2 266 932	35 967 345	365 319 349	7.175×10^{-8}

[a]Observed values from Table I, interpolated and extrapolated with predicted values from Table I.
[b]Obtained from the formula of Edlén, Ref. [43].
[c]Interpolated numerical calculations of Johnson et al., Ref. [44].

ments of lower precision but higher charge for both intervals for $Z = 54$ [38], and for the irregular-doublet interval for $Z = 92$ [39]. Thus, a charge screening $\cong 0.9$ in the hydrogenlike Lamb shift reproduces the residue between measured and RMBPT calculated values for the irregular-doublet interval to within measurement uncertainties for $10 \le Z \le 92$. Similarly, accurate representations are obtained with a screening $\cong 1.4$ for the regular-doublet interval, although here the interval is less sensitive to the Lamb shift.

Table II summarizes the excitation energies used in the calculation of transition probabilities. Here the measured values are used where available, and the parametrized values of Table I are used where no measurements exist.

The ionization potentials were computed by an extension of the semiempirical formula of Edlén [43]. Since this formula was developed primarily for interpolation and smoothing for $Z \le 28$, the validity of the extrapolation to high Z required verification. We therefore performed *ab initio* calculations using the MCDF program

developed Grant and co-workers [49]. We found that the extrapolations of the Edlén formula agree with the MCDF calculations to within better than 0.2% for $74 \le Z \le 92$. The former were adopted for use here and are listed in Table II. The dipole polarizabilities for the heliumlike core were obtained by an interpolation of the calculations of Johnson, Kolb, and Huang [44], and are also listed in Table II.

A critical compilation of lifetime measurements for the $2p$ levels for ions in the Li sequence has been made and the values selected are listed in Table III. Both measurements listed for neutral Li were made using selective excitation of an atomic beam by a laser, one by time-of-flight [10] and the other by delayed-coincidence [11] methods. All of the measurements listed for charged ions were made using beam-foil excitation methods. The compilation gives precedence to studies that reported the lifetimes of both $2p$ levels. These experimental lifetimes, their source references, and their quoted uncertainties are given in Table III.

TABLE III. Theoretical and experimental lifetimes for $2p_{1/2,3/2}$ levels and oscillator strengths for the $2s$-$2p_{1/2,3/2}$ transitions of the Li isoelectronic sequence. Errors in the experimental values are indicated in parentheses.

Ion	Z	τ (ns) $2p_{1/2}$ Calc.	$2p_{1/2}$ Expt.	$2p_{3/2}$ Calc.	$2p_{3/2}$ Expt.
Li	3	27.304 96	27.29(4)[a] 27.22(20)[b]	27.303 14	
Be	4	8.929 33		8.923 22	8.1(4)[c] 9.29(20)[d]
B	5	5.333 73		5.321 54	5.6(3)[c]
C	6	3.829 86	3.68(9)[e]	3.809 47	3.69(10)[e]
N	7	2.997 53	3.20(15)[f] 3.08(15)[g] 3.17(9)[h]	2.967 06	3.20(5)[f] 3.12(15)[g] 3.17(9)[h]
O	8	2.465 40	2.66(9)[e] 2.51(10)[i] 2.7(2)[j]	2.423 01	2.56(7)[e] 2.47(10)[i] 2.4(2)[j]
F	9	2.094 45	2.04(9)[f]	2.038 32	2.04(9)[f]
Ne	10	1.820 16	1.88(9)[e] 1.51(40)[k]	1.748 90	1.86(9)[e] 1.47(40)[k]
Na	11	1.608 68		1.520 58	
Mg	12	1.440 27		1.334 69	
Al	13	1.302 84	1.35(6)[l]	1.178 54	1.19(5)[l]
Si	14	1.188 56	1.20(4)[m] 1.00(8)[n]	1.044 98	1.07(4)[m] 1.12(8)[n] 1.01(10)[o]
P	15	1.091 95		0.928 38	
S	16	1.008 76	0.918(92)[p]	0.825 93	0.767(39)[p]
Cl	17	0.936 53	0.95(5)[q] 1.0(1)[r]	0.734 76	0.76(4)[q] 0.71(3)[r]
Ar	18	0.873 36		0.652 74	
K	19	0.817 46		0.579 08	
Ca	20	0.767 52		0.512 58	
Sc	21	0.722 76		0.452 65	
Ti	22	0.682 02		0.398 58	
V	23	0.645 57		0.349 91	
Cr	24	0.611 94		0.306 18	
Mn	25	0.581 00		0.266 98	
Fe	26	0.552 85	0.55(2)[s]	0.232 23	0.235(10)[s]
Co	27	0.526 92		0.201 41	
Ni	28	0.502 66		0.174 03	
Cu	29	0.480 18		0.149 99	
Zn	30	0.459 18		0.128 94	
Ga	31	0.439 52		0.110 54	
Ge	32	0.421 08		0.094 54	
As	33	0.403 75		0.080 69	
Se	34	0.387 38		0.068 74	
Br	35	0.372 10		0.058 46	
Kr	36	0.357 52	0.32(3)[t]	0.049 64	0.052(3)[t]
Rb	37	0.343 79		0.042 11	
Sr	38	0.330 80		0.035 68	
Y	39	0.318 43		0.030 21	
Zr	40	0.306 60		0.025 56	
Nb	41	0.295 24		0.021 61	

TABLE III. (*Continued*).

Ion	Z	τ (ns) $2p_{1/2}$ Calc.	Expt.	$2p_{3/2}$ Calc.	Expt.
Mo	42	0.284 54		0.018 28	
Tc	43	0.274 32		0.015 45	
Ru	44	0.264 73		0.013 06	
Rh	45	0.255 64		0.011 05	
Pd	46	0.246 73		0.009 35	
Ag	47	0.238 27		0.007 91	
Cd	48	0.230 12		0.006 70	
In	49	0.222 24		0.005 68	
Sn	50	0.214 62		0.004 81	
Sb	51	0.207 22		0.004 08	
Te	52	0.200 03		0.003 46	
I	53	0.193 04		0.002 94	
Xe	54	0.186 23		0.002 50	
Cs	55	0.179 70		0.002 12	
Ba	56	0.173 48		0.001 81	
La	57	0.167 52		0.001 54	
Ce	58	0.161 81		0.001 32	
Pr	59	0.156 37		0.001 13	
Nd	60	0.151 10		0.000 96	
Pm	61	0.146 03		0.000 83	
Sm	62	0.141 15		0.000 71	
Eu	63	0.136 46		0.000 61	
Cd	64	0.131 95		0.000 52	
Tb	65	0.127 60		0.000 45	
Dy	66	0.123 41		0.000 39	
Ho	67	0.119 37		0.000 34	
Er	68	0.115 47		0.000 29	
Tm	69	0.111 72		0.000 25	
Yb	70	0.108 10		0.000 22	
Lu	71	0.104 60		0.000 19	
Hf	72	0.101 23		0.000 16	
Ta	73	0.097 98		0.000 14	
W	74	0.094 90		0.000 12	
Re	75	0.091 88		0.000 11	
Os	76	0.088 99		0.000 092	
Ir	77	0.086 22		0.000 080	
Pt	78	0.083 56		0.000 070	
Au	79	0.081 01		0.000 061	
Hg	80	0.078 56		0.000 053	
Tl	81	0.076 21		0.000 046	
Pb	82	0.073 96		0.000 041	
Bi	83	0.071 79		0.000 035	
Po	84	0.069 72		0.000 031	
At	85	0.067 73		0.000 027	
Rn	86	0.065 81		0.000 024	
Fr	87	0.063 98		0.000 021	
Ra	88	0.062 28		0.000 019	
Ac	89	0.060 59		0.000 016	

TABLE III. (*Continued*).

		τ (ns)			
		$2p_{1/2}$		$2p_{3/2}$	
Ion	Z	Calc.	Expt.	Calc.	Expt.
Th	90	0.058 97		0.000 014	
Pa	91	0.057 42		0.000 013	
U	92	0.055 92		0.000 011	

[a]Gaupp et al., Ref. [10].
[b]Carlsson and Sturesson, Ref. [11].
[c]Andersen et al., Ref. [12] (multiplet value).
[d]Bergström et al., Ref. [13] (multiplet value).
[e]Knystautas et al., Ref. [14].
[f]Barrette et al., Ref. [15].
[g]Kernahan et al., Ref. [16].
[h]Bickel et al., Ref. [17].
[i]Pinnington et al., Ref. [18].
[j]Martinson et al., Ref. [19].

[k]Buchet et al., Ref. [20].
[l]Denne et al., Ref. [21].
[m]Livingston et al., [Ref. 22].
[n]Träbert et al., Ref. [23].
[o]Pegg et al., Ref. [24].
[p]Pegg et al., Ref. [25].
[q]Forester et al., Ref. [26].
[r]Ishii et al., Ref. [27].
[s]Dietrich et al., Ref. [28].
[t]Dietrich et al., Ref. [29].

III. METHOD OF WAVE-FUNCTION AND MATRIX-ELEMENT CALCULATION

The calculational approach used in this paper was detailed in Ref. [32] and has been modified slightly since then. Basically we use a numerical extension of the Coulomb approximation whereby the finite core of the atom or ion is represented, in general, by a model (central) potential (CAMP) or by a self-consistent Hartree-Slater (CAHS) or Dirac-Slater (CADS) potential. Additional effects of electron-core interactions such as core polarization and spin-orbit interaction are also included (see Ref. [32] for details and a discussion of the various forms). The Schrödinger equation for the valence electron is solved numerically by *inward* integration. The experimental or semiempirical values for both the excitation energy and the ionization limit are used as inputs in specifying the binding energy. This energy is held constant and no iteration is made. The inward integration is matched with an outward integration at the *inner* classical turning point. A discontinuity in the derivative of the wave function occurs at the matching point, but the effects of this are insignificant for the purposes of the present calculation.

Experience with calculations in the Na and Cu isoelectronic sequences [30,31] has shown that, because of its inward and the noniterative nature, the results of this approach have minimal dependence on the polarization-potential term in the Schrödinger equation. In addition, there is a degree of uncertainty about the necessary cutoff distances in such a potential, although some reasonable choices can be made [30]. Using a model potential (i.e., a potential that has parameters adjusted to fit the observed energy), binding energies may not yield the most accurate (in shape) wave functions, and this creates ambiguities in the choice of the cutoff radii for the polarization potentials and core-polarization corrections to the dipole operator.

Experience [30–33] has also shown that the most

prominent effect of the core polarizability is on the dipole-moment operator, which can be written as [32,35]

$$d = e \left[r - \alpha_d \frac{\mathbf{r}}{r^3} \left\{ 1 - \exp\left[-\left[\frac{r}{r_c} \right]^3 \right] \right\} \right] , \qquad (1)$$

where α_d is the dipole polarizability of the core (in this case heliumlike). The cutoff factor in the curly brackets (with a cutoff radius r_c) has been chosen as the most physical type [32].

Based on the above experience, and to remove some of the earlier uncertainties in the various cutoff distances, both in the polarization potential and in the dipole-matrix element, we have consistently made the following choices.

(a) The potential used in the Schrödinger equation was

$$V(r) = V_{HS}(r) + V_{s.o.}(r) , \qquad (2)$$

$$V_{s.o.}(r) = \frac{(\alpha^2/2)\mathbf{l}\cdot\mathbf{s}}{\{1 + (\alpha^2/2)[E - V_{HS}(r)]\}^2} \frac{1}{r} \frac{dV_{HS}}{dr} , \qquad (3)$$

where V_{HS} is the Hartree-Slater potential [34] of the ground state of the atom or ion and $V_{s.o.}$ is the spin-orbit potential. Notice that the polarization potential was totally omitted.

(b) The cutoff radius used in the dipole matrix element [of Eq. (3)] is the Hartree-Slater radius of the ion core.

As a result of these choices, our calculations have semiempirical dependence on only the input energy levels and the dipole polarizabilities (taken from Ref. [44]), and have *no* adjustable parameters. Thus, they provide unique predictions of lifetime and oscillator strengths.

IV. RESULTS AND DISCUSSION

Figure 2 displays a plot of our CAHS calculations of the charge-scaled line strengths $Z^2 S(2s - 2p_J)$ for the $J = \frac{1}{2}$ and $\frac{3}{2}$ transitions, plotted versus the reciprocal

TABLE IV. Absorption oscillator strengths f computed by the semiempirical Coulomb approximation with realistic model potential compared with selected *ab initio* calculations.

			f				
			$2s$-$2p_{1/2}$			$2s$-$2p_{3/2}$	
Ion	Z	CAHS[a]	CKD[b]	AFL[c]	CAHS[a]	CKD[b]	AFL[c]
Li	3	0.247 15	0.255 2	0.255	0.494 31	0.510 4	0.511
Be	4	0.164 67	0.171 5	0.171	0.329 44	0.343 1	0.343
B	5	0.120 18	0.124 8	0.125	0.240 58	0.249 9	0.250
C	6	0.094 13	0.097 36	0.097	0.188 64	0.195 1	0.195
N	7	0.077 24	0.079 59	0.079	0.155 08	0.159 8	0.160
O	8	0.065 47	0.067 23	0.067	0.131 77	0.135 3	0.135
F	9	0.056 79	0.058 16	0.058	0.114 71	0.117 5	0.118
Ne	10	0.050 15	0.051 24	0.051	0.101 75	0.104 0	0.104
Na	11	0.044 90	0.045 79		0.091 63	0.093 43	
Mg	12	0.040 65	0.041 38		0.083 54	0.085 03	
Al	13	0.037 14	0.037 75		0.077 00	0.078 22	
Si	14	0.034 19	0.034 71		0.071 56	0.072 62	
P	15	0.031 68	0.032 12		0.067 08	0.067 98	
S	16	0.029 52	0.029 89		0.063 32	0.064 10	
Cl	17	0.027 64	0.027 96		0.060 17	0.060 85	
Ar	18	0.025 98	0.026 26	0.026	0.057 52	0.058 11	0.058
K	19	0.024 52	0.024 76		0.055 29	0.055 81	
Ca	20	0.023 22	0.023 42		0.053 42	0.053 87	
Sc	21	0.022 05	0.022 23		0.051 86	0.052 26	
Ti	22	0.021 00	0.021 15		0.050 58	0.050 92	
V	23	0.020 04	0.020 17		0.049 53	0.049 83	
Cr	24	0.019 17	0.019 28		0.048 70	0.048 96	
Mn	25	0.018 38	0.018 47		0.048 07	0.048 28	
Fe	26	0.017 65	0.017 73	0.018	0.047 60	0.047 78	0.048
Co	27	0.016 97	0.017 04		0.047 29	0.047 43	
Ni	28	0.016 35	0.016 40		0.047 13	0.047 24	
Cu	29	0.015 78	0.015 82		0.047 10	0.047 18	
Zn	30	0.015 24	0.015 27		0.047 20	0.047 25	
Ga	31	0.014 75			0.047 42		
Ge	32	0.014 28			0.047 75		
As	33	0.013 85			0.048 16		
Se	34	0.013 44			0.048 72		
Br	35	0.013 06	0.013 05		0.049 35	0.049 25	
Kr	36	0.012 70	0.012 68		0.050 07	0.049 93	
Rb	37	0.012 36			0.050 88		
Sr	38	0.012 04			0.051 77		
Y	39	0.011 74			0.052 74		
Zr	40	0.011 45			0.053 80		
Nb	41	0.011 18	0.011 13		0.054 93	0.054 61	
Mo	42	0.010 92	0.010 86	0.011	0.056 14	0.055 78	0.056
Tc	43	0.010 68			0.057 43		
Ru	44	0.010 44			0.058 78		
Rh	45	0.010 22			0.060 19		
Pd	46	0.010 01			0.061 68		
Ag	47	0.009 80			0.063 24		
Cd	48	0.009 61	0.009 53		0.064 87	0.064 24	
In	49	0.009 42			0.066 57		
Sn	50	0.009 24			0.068 35		
Sb	51	0.009 08			0.070 19		
Te	52	0.008 92			0.072 12		
I	53	0.008 76	0.008 65		0.074 11	0.073 12	
Xe	54	0.008 62	0.008 50		0.076 19	0.075 08	
Cs	55	0.008 48			0.078 32		
Ba	56	0.008 34			0.080 52		
La	57	0.008 21			0.082 77		
Ce	58	0.008 08			0.085 08		
Pr	59	0.007 96	0.007 81		0.087 46	0.085 85	

TABLE IV. (Continued).

			f				
			$2s\text{-}2p_{1/2}$			$2s\text{-}2p_{3/2}$	
Ion	Z	CAHS[a]	CKD[b]	AFL[c]	CAHS[a]	CKD[b]	AFL[c]
Nd	60	0.007 84			0.089 89		
Pm	61	0.007 72			0.092 39		
Sm	62	0.007 61			0.094 95		
Eu	63	0.007 50			0.097 58		
Gd	64	0.007 40	0.007 22		0.100 28	0.098 17	
Tb	65	0.007 30			0.103 05		
Dy	66	0.007 20			0.105 89		
Ho	67	0.007 10			0.108 84		
Er	68	0.007 01			0.111 83		
Tm	69	0.006 92	0.006 72		0.114 90	0.112 1	
Yb	70	0.006 83			0.118 05		
Lu	71	0.006 74			0.121 28		
Hf	72	0.006 65			0.124 60		
Ta	73	0.006 57			0.128 01		
W	74	0.006 49	0.006 28	0.007 1	0.131 51	0.127 5	0.129
Re	75	0.006 41			0.135 10		
Os	76	0.006 33			0.138 77		
Ir	77	0.006 25			0.142 51		
Pt	78	0.006 18			0.146 33		
Au	79	0.006 10	0.005 88		0.150 24	0.144 6	
Hg	80	0.006 03	0.005 80		0.154 21	0.148 3	
Tl	81	0.005 95			0.158 27		
Pb	82	0.005 88	0.005 65		0.162 40	0.155 7	
Bi	83	0.005 81			0.166 60		
Po	84	0.005 74			0.170 88		
At	85	0.005 67			0.175 23		
Rn	86	0.005 60			0.179 66		
Fr	87	0.005 53			0.184 15		
Ra	88	0.005 46			0.188 72		
Ac	89	0.005 39			0.193 35		
Th	90	0.005 32			0.198 05		
Pa	91	0.005 26			0.202 81		
U	92	0.005 19	0.004 87	0.062	0.207 64	0.197 0	0.200

[a]This work, Coulomb approximation with Hartree-Slater core.
[b]Cheng, Kim, and Desclaux, Ref. [3], MCDF calculation.
[c]Armstrong, Fielder, and Lin, Ref. [2], MCDF calculation.

screened charge $1/(Z-2.17)$. The empirical screening constant was chosen to be 2.17 rather than 2.0 (the number of core electrons) to enhance the linearity of the plot. This overscreening may indicate the presence of exchange-core-polarization [53] effects in this sequence. The apparent linearity over most of the sequence, with a sudden downturn at a high value of Z, is characteristic of line strengths for a wide variety of atomic systems when presented on the type of isoelectronic plot [54]. As can be seen from the inset in Fig. 2, the apparent linearity persists for nearly 40 states of ionization, which is similar to the behavior noted for the Na [30] and Cu [31] sequences. While there is presently no theoretical explanation for the existence of this linearity, it provides a useful tool for the interpolation and extrapolation of measured and computed values [54].

In the nonrelativistic limit, the ratio of these two line strengths would be exactly two, and the ratio of the two lifetimes would be proportional to the cube of the wavelength ratio. Our calculations indicate that the line-strength ratio varies from 2.0 for neutral Li to 2.5 for U^{+89}, with the increment above 2.0 being nearly proportional to the square of the degree of ionization.

The isoelectronic regularities in the line strengths and their ratios can provide a means for relating the lifetimes of the $J=\frac{1}{2}$ and $\frac{3}{2}$ levels in regions of differing experimental accessibility. Lifetimes in the range between ps and fs are difficult to measure directly, since the decay length (0.3 mm/ps at $v=c$) is too short to be measured by time-of-flight methods and the full width at half maximum of natural line width Γ_{FWHM} (eV)$=0.66/\tau$(fs) is too narrow to be determined spectroscopically. Isoelectronic information concerning the longer-lived $J=\frac{1}{2}$ level could thus be combined with extrapolated ratios to infer rate constants for the $J=\frac{3}{2}$ transitions.
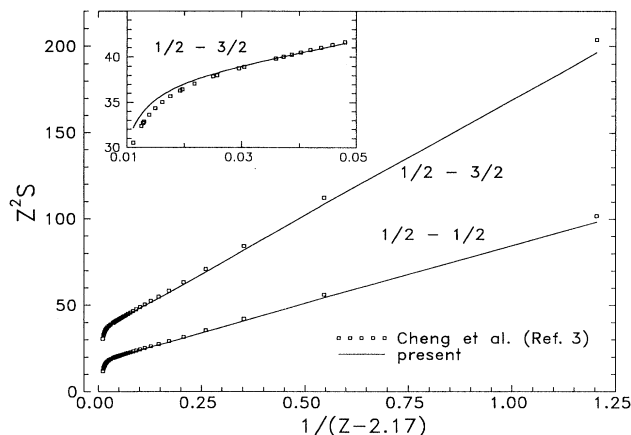
FIG. 2. Plot of the charge-scaled line $Z^2S(2s\text{-}2p_J)$ vs the reciprocal effective screened charge $1/(Z-2.17)$ for the $J=\frac{1}{2}$ and $\frac{3}{2}$ intervals. The inset magnifies the region $20 \le Z \le 92$ and indicates that the apparent linearity persists for almost 40 stages of ionization.
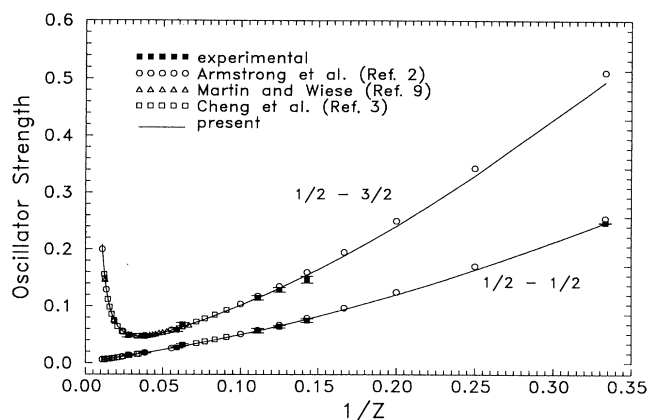

FIG. 3. Plot of experimental and theoretical values for the absorption oscillator strengths vs reciprocal nuclear charge. Solid lines trace the calculations reported here, open circles and open squares denote the *ab initio* calculations of Armstrong *et al.* [2] and Cheng *et al.* [3], and open triangles denote the critical compilation of Martin and Wiese [9]. The experimental measurements [10–29] are dénoted by solid squares, with their quoted uncertainties spanned by error bars.

Our calculations of lifetimes and oscillator strengths for $n=2$ levels are presented in Table III and compared with experimental values. Table IV lists the values of the absorption oscillator strengths obtained from the semiempirical CAHS method, and compares them to *ab initio* calculations. Figure 3 presents the CAHS, *ab initio*, and critically compiled values for the absorption oscillator strength, plotted versus the reciprocal nuclear charge.

Experimental and *ab initio* theoretical lifetime results for neutral alkali-metal atoms have exhibited an interesting set of discrepancies, which the semiempirical calculations presented here may serve to elucidate. Results for the neutral Li, Na, and Cu atoms are summarized in Table V. Highly precise beam-laser lifetime measure-

ments have been performed by Gaupp *et al.* [10], Schmoranzer *et al.* [55], and Carlsson *et al.* [11,56,57] which yield lifetimes that are significantly longer than the best available *ab initio* theoretical values [58–61]. This has caused controversy, and doubts have been raised [4] whether uncertainties in the *ab initio* calculations can accommodate these discrepancies.

As can be seen from Table V, our semiempirical calculations agree very well with the experimental results, and thereby consistently (albeit on a 1% level) disagree with the *ab initio* results. This is puzzling, since the *ab initio* calculations are expected to be very reliable for these systems. Since our semiempirical computation of lifetimes uses exactly the same procedures for the Li, Na, and Cu

TABLE V. Comparison of measured, semiempirically computed, and *ab initio* computed valued for the lifetimes τ of the ns-np resonance transitions in neutral Li, Na, and Cu atoms.

Atom	Transition	Gaupp[a]	Schmoranzer[b]	Carlsson[c]	CAHS[d]	MCHF[e]	MBPT[f]	MBPT[g]
							Ab initio theory	
Li	$2s(1/2)\text{-}2p(1/2)$	27.29(4)		27.20(20)	27.305	27.07	27.04	
	$2s(1/2)\text{-}2p(3/2)$				27.303			
Na	$3s(1/2)\text{-}3p(1/2)$	16.40(3)	16.40(5)	16.38(8)	16.399	16.12	16.11	16.24
	$3s(1/2)\text{-}3p(3/2)$		16.35(5)	16.36(20)	16.352	16.07	16.07	16.19
Cu	$4s(1/2)\text{-}4p(1/2)$			7.27(6)	7.251	6.87		
	$4s(1/2)\text{-}4p(3/2)$			7.17(6)	7.069	6.68		

[a]Reference [10].
[b]Reference [55].
[c]Li, Ref. [11]; Na, Ref. [56]; Cu, Ref. [57].
[d]Li, this work; Na, Ref. [30]; Cu, Ref. [31].
[e]Li and Na, Fischer, Ref. [58]; Cu, Carlsson, Ref. [59].
[f]Johnson *et al.*, Ref. [60].
[g]Guet *et al.*, Ref. [61].

sequences, is uniquely specified by the empirical energy level data, and has no free parameters to adjust, there can be no unconscious bias toward the experimental lifetime data. Furthermore, the semiempirical approach forces the wave functions to yield the correct experimental energies, whereas the *ab initio* wave functions tend to systematically underestimate the experimental binding energies by a few percent. However, the *ab initio* calculations [58–61] have been carried out with great care, and their discrepancy with the experimental and semiempirical results remains an enigma.

V. CONCLUSIONS

The systemization described here brings several methods to bear upon transition-probability specification. The CAHS method provides accurate predictions of tran-

sition probabilities, but requires spectroscopic data. If comprehensive wavelength measurements are not available, existing data can be semiempirically parametrized and extrapolated, a procedure which can be aided by *ab initio* spectroscopic calculations. These can be semiempirically adjusted to match experimental trends, then inserted into the Hartree-Slater program to produce semiempirical wave functions that yield transition rates superior to those obtained by fully *ab initio* methods.

[1] Y.-K. Kim and J. P. Desclaux, Phys. Rev. Lett. **36**, 139 (1976).

[2] L. Armstrong, Jr., W. R. Fielder, and D. L. Lin, Phys. Rev. A **14**, 1114 (1976).

[3] K.-T. Cheng, Y.-K. Kim, and J. P. Desclaux, At. Data Nucl. Data Tables **24**, 111 (1979).

[4] R. P. McEachran and M. Cohen, J. Phys. B **16**, 3125 (1983).

[5] E. Biémont, Astron. Astrophys. Suppl. **27**, 489 (1977).

[6] A. Lindgård and S. E. Nielsen, At. Data Nucl. Data Tables **19**, 533 (1977).

[7] C. Barrientos and I. Martin, Phys. Rev. A **42**, 432 (1990).

[8] W. L. Wiese, M. W. Smith, and B. M. Miles, in *Atomic Transition Probabilities*, Natl. Bur. Stand (U.S.) Circ. No. 22 (U.S. GPO, Washington, DC, 1969), Vol. 2.

[9] G. A. Martin and W. L. Wiese, J. Phys. Chem. Ref. Data **5**, 537 (1976); Phys. Rev. A **13**, 699 (1974).

[10] A. Gaupp, P. Kuske, and H. J. Andrä, Phys. Rev. A **26**, 3351 (1982).

[11] J. Carlsson and L. Sturesson, Z. Phys. D **14**, 281 (1989).

[12] T. Andersen, K. A. Jessen, and G. Sørensen, Phys. Lett. **29A**, 384 (1969).

[13] I. Bergström, J. Bromander, R. Buchta, L. Lundin, and I. Martinson, Phys. Lett. **28A**, 721 (1969).

[14] E. J. Knystautas, L. Barrette, B. Neveu, and R. Drouin, J. Quant. Spectrosc. Radiat. Transfer **11**, 75 (1971).

[15] L. Barrette, E. J. Knystautas, B. Neveu, and R. Drouin, Phys. Lett. **32A**, 435 (1970).

[16] J. A. Kernahan, A. E. Livingston, and E. H. Pinnington, Can. J. Phys. **52**, 1895 (1974).

[17] W. S. Bickel, H. G. Berry, J. Désesquelles, and S. Bashkin, J. Quant. Spectrosc. Radiat. Transfer **9**, 1145 (1969).

[18] E. H. Pinnington, D. J. G. Irwin, A. E. Livingston, and J. A. Kernahan, Can. J. Phys. **52**, 1961 (1974).

[19] I. Martinson, H. G. Berry, W. S. Bickel, and H. Oona, J. Opt. Soc. Am. **61**, 519 (1971).

[20] J. P. Buchet, M. C. Buchet-Poulizac, G. Do Cao, and J. Désesquelles, Nucl. Instrum. Methods **110**, 19 (1973).

[21] B. Denne, D. J. Pegg, K. Ishii, E. Alvarez, R. Hallin, J. Pihl, and R. Sjödin, J. Phys. (Paris) Colloq. **40**, C1-183 (1979).

[22] A. E. Livingston, F. G. Serpa, A. S. Zacarias, L. J. Curtis, H. G. Berry, and S. A. Blundell, Phys. Rev. A (to be pub-

lished).

[23] E. Träbert, P. H. Heckmann, and H. v. Buttlar, Z. Phys. A **281**, 333 (1977).

[24] D. J. Pegg, P. M. Griffin, G. D. Alton, S. B. Elston, J. P. Forester, M. Suter, R. S. Thoe, C. R. Vain, and B. M. Johnson, Phys. Scr. **18**, 18 (1978).

[25] D. J. Pegg, J. P. Forester, C. R. Vane, S. B. Elston, P. M. Griffin, K.-O. Groeneveld, R. S. Peterson, R. S. Thoe, and I. A. Sellin, Phys. Rev. A **15**, 1958 (1977).

[26] J. P. Forester, D. J. Pegg, P. M. Griffin, G. D. Alton, S. B. Elston, H. C. Hayden, R. S. Thoe, C. R. Vane, and J. J. Wright, Phys. Rev. A **18**, 1476 (1978).

[27] K. Ishii, E. Alvarez, R. Hallin, J. Lindskog, A. Marelius, J. Pihl, R. Sjödin, B. Denne, L. Engström, S. Huldt, and I. Martinson, Phys. Scr. **18**, 57 (1978).

[28] D. D. Dietrich, J. A. Leavitt, S. Bashkin, J. G. Conway, H. Gould, J. Gould, D. MacDonald, R. Marrus, B. M. Johnson, and D. J. Pegg, Phys. Rev. A **18**, 208 (1978).

[29] D. D. Dietrich, J. A. Leavitt, H. Gould, and R. Marrus, Phys. Rev. A **22**, 1109 (1980).

[30] C. E. Theodosiou and L. J. Curtis, Phys. Rev. A **38**, 4435 (1988).

[31] L. J. Curtis and C. E. Theodosiou, Phys. Rev. A **39**, 605 (1989).

[32] C. E. Theodosiou, Phys. Rev. A **30**, 2881 (1984).

[33] C. E. Theodosiou, Phys. Rev. A **30**, 2910 (1984).

[34] J. P. Desclaux, Comput. Phys. Commun. **1** 216 (1969).

[35] I. Bersuker, Opt. Spektrosk. **3**, 97 (1957); S. Hameed, A. Herzenberg, and M. G. James, J. Phys. B **1**, 822 (1968).

[36] B. Edlén, Phys. Scr. **28**, 51 (1983).

[37] E. Hinnov and B. Denne, Phys. Rev. A **40**, 4357 (1989).

[38] S. Martin, J. P. Buchet, M. C. Buchet-Poulizac, A. Denis, J. Désesquelles, M. Druetta, J. P. Grandin, D. Hennecart, X. Husson, and D. Lecler, Europhys. Lett. **10**, 645 (1989).

[39] J. Schweppe, A. Belkacem, L. Blumenfeld, N. Claytor, B. Feinberg, H. Gould, V. Kostroun, L. Levy, S. Misawa, R. Mowat, and M. Prior, Bull. Am. Phys. Soc. **35**, 1178 (1990).

[40] S. Martin, A. Denis, M. C. Buchet-Poulizac, J. P. Buchet, and J. Desesquelles, Phys. Rev. A **42**, 6570 (1990).

[41] B. Denne-Hinnov, Phys. Rev. A (to be published).

[42] L. J. Curtis, Phys. Scr. **39**, 447 (1989).

[43] B. Edlén, Phys. Scr. **19**, 255 (1979) (footnote d of Table VI

and footnote a of Table I).

[44] W. R. Johnson, D. Kolb and K.-N. Huang, At. Data Nucl. Data Tables **28**, 333 (1983).

[45] W. R. Johnson, S. A. Blundell, and J. Sapirstein, Phys. Rev. A **37**, 2764 (1988).

[46] S. A. Blundell, W. R. Johnson, and J. Sapirstein, Phys. Rev. A **41**, 1698 (1990).

[47] P. Indelicato and J. P. Desclaux, Phys. Rev. A **42**, 5139 (1990).

[48] J. P. Desclaux, K. T. Cheng, and Y.-K. Kim, J. Phys. B **12**, 3819 (1979).

[49] I. P. Grant, B. J. McKenzie, P. H. Norrington, D. F. Mayers, and N. C. Pyper, Comput. Phys. Common. **21**, 207 (1980); K. G. Dyall, I. P. Grant, C. T. Johnson, F. A. Parpia, and E. P. Plummer, *ibid*. **55**, 425 (1989).

[50] P. J. Mohr, Ann. Phys. (NY) **88**, 52 (1974); Phys. Rev. Lett. **34**, 1050 (1975).

[51] J. F. Seely, Phys. Rev. A **39**, 3682 (1989).

[52] W. R. Johnson and G. Soff, At. Data Nucl. Data Tables **33**, 405 (1985).

[53] J. Wangler, L. Henke, W. Wittmann, H. J. Plöhn, and H. J. Andrä, Z. Phys. A **299**, 23 (1981).

[54] L. J. Curtis, Phys. Scr. **43**, 137 (1991).

[55] H. Schmoranzer, D. Schulze-Hagenest, and S. A. Kandela (unpublished).

[56] J. Carlsson, Z. Phys. D **9**, 147 (1988).

[57] J. Carlsson, L. Sturesson, and S. Svanberg, Z. Phys. D **11**, 287 (1989).

[58] C. Froese Fischer, Nucl. Instrum. Methods Phys. Res. B **31**, 265 (1988).

[59] J. Carlsson, Phys. Rev. A **38**, 1702 (1988).

[60] W. R. Johnson, M. Idrees, and J. Sapirstein, Phys. Rev. A **35**, 3218 (1987).

[61] C. Guet, S. A. Blundell, and W. R. Johnson, Phys. Lett. A **143**, 384 (1990).